Computational Condensed Matter 9 (2016) 27–34

Contents lists available at ScienceDirect

Computational Condensed Matter

journal homepage: http://ees.elsevier.com/cocom/default.asp

Relaxation dynamics and growth modes of metastable spin-crossover materials with magnetic interactions

T.D. Oke [a], F. Hontinfinde [a, *], K. Boukheddaden [b]

[a] Département de Physique (FAST) et Institut des Mathématiques et de Sciences Physiques (IMSP), Université d'Abomey-Calavi, 01 BP 613 Porto-Novo, Benin
[b] Groupe d'Etudes de la matiére condensée, Université Paris-Saclay, Université de Versailles/St. Quentin en Yvelines-CNRS, 45 Avenue des Etats Unis., F78035 Versailles Cedex, France

ARTICLE INFO

Article history:
Received 21 June 2016
Received in revised form
9 August 2016
Accepted 18 September 2016
Available online 4 October 2016

Keywords:
Spin-crossover compounds
Relaxation dynamics
Monte Carlo simulations
2*D*-nucleation
Growth phase diagram

ABSTRACT

A two-dimensional spin-1 Blume-Emery-Griffiths (BEG) model is used to describe the relaxation dynamics of spin-crossover (SC) compounds with magnetic interactions from a metastable high-spin state by means of Monte Carlo simulations with Arrhenius dynamics. The model comprises temperature-dependent effective spin exchange interaction accounting for spin-phonon interactions. The growth modes of the stable low-spin state domains are singled out in the model parameters' space. For weak magnetic interactions, numerical results indicated a kind of 2*D*-nucleation with the birth, spread and coalescence of low-spin diamagnetic domains following the Becker-Doering law. A schematic growth phase diagram is presented.

1. Introduction

Metastable states can be found in various areas in physics: supercooled fluids [1], crystal surface growth [2], ferroelectrics [3], vortex states in superconductors [4], etc. The study of the growth and decay kinetics of these states has attracted much interest from scientists in a wide variety of basic and applied contexts for several decades [5]. For instance, the growth kinetics of metastable (331) nanofacets on Au(110) and Pt(110) surfaces has been investigated by Ndongmouo et al. [6] from a theoretical point of view. They realized that this growth proceeds via 2*D*-nucleation mechanism at low temperature in the submonolayer regime. In this paper, we address the problem of decay of metastability in spin-crossover (SC) compounds and Prussian Blue Analogs (PBAs) which are known to display fascinating physical properties investigated by several authors (see Ref. [7]). It is known that these materials are bistable solids and are potential candidates for technological applications, in particular as displays and information storage devices. SC materials can generate a molecular magnetism where the spin state and the magnetic moment of the central iron $F_e^{(II)}$ *d* block ion can be changed or controlled by external constraints as temperature, light, magnetic field, pressure, etc [8,9]. Under special short-time constraints, the system may reach a saturated metastable high-spin (HS) state and then relaxes back to the low-spin (LS) state (see Refs. [9–11] and references therein). Sigmoidal relaxation curves of the HS fraction are often got and their behavior strongly depends on values of the model parameters. Here, we are interested in the spin-transition systems with magnetic interactions. Then, our investigations are focused on the growth kinetics and modes of the stable diamagnetic (LS) phase. This structure growth problem from metastable state, can exactly be mapped onto the submonolayer growth problem of a two-dimensional crystal [12]. In this context, the study of the key factors determining the growing island shapes is essential for getting insight on the growth modes and atomic manipulation for new compounds for technological applications. This interest stimulated much theoretical works in the past [13,14]. The tools for these investigations are Monte Carlo (MC) simulations [15,16] and rate equations (RE) theory [17,18]. By means of the RE theory, reliable predictions are possible on monomer (isolated growth unit) and island densities together with their size distribution or average size. Using MC simulations, one can easily study the finite extension of islands and

* Corresponding author.
E-mail address: fhontinfinde@yahoo.fr (F. Hontinfinde).

http://dx.doi.org/10.1016/j.cocom.2016.09.003

coalescence phenomena at high coverages. In general, during the growth, supercritical nuclei of the "new phase" are formed. They extend and further coalesce to form "a macroscopic domain" of the new phase. We show in this work that under suitable physical conditions, the decay of the metastable HS phase proceeds via 2*D*-nucleation of stable LS nuclei. Indeed, the calculated mean growth velocity of the LS phase follows the Becker-Doering law at weak magnetic interactions [7]. The dynamics through which the relaxation occurs is driven by thermal fluctuations.

In section 2, the model is described and the simulation procedure is presented. Section 3 is devoted to numerical results and discussions. Section 4 contains the conclusion of the work.

2. Model and simulation procedure

The model is defined on a 2*D* square lattice with periodic boundary conditions. The Hamiltonian considered for the system energetics reads:

$$H = -J \sum_{<i,j>} s_i s_j - K \sum_{<i,j>} s_i^2 s_j^2 + D \sum_i s_i^2 \quad (1)$$

where the spin $s_i = 0,\pm 1$ is located at site i of the lattice; $<i,j>$ denotes nearest-neighbors (nn) pairs. J is the nearest-neighbor effective magnetic exchange coupling constant. The parameters K and D are the quadrupolar interaction and the effective ligand-field strength, respectively. An important parameter considered in the calculations is the ratio $\gamma = J/K$. When $\gamma = 0$, magnetic interactions are absent in the model. The first sum runs over interacting nn. The second one represents the biquadratic isotropic exchange interactions. The third term is the single ion anisotropy. The effective ligand-field strength, D, is assumed to depend on the absolute temperature T of the system, the degeneracy ratio g between LS and HS states and the ligand-field energy splitting Δ. The quadrupolar interaction, K, is assumed to be proportional to the absolute temperature in view to account for spin-phonon coupling contributions to SC materials' properties. These parameters are defined as: $K = \alpha k_B T$ and $D = \Delta - k_B T \ln(g)$ (see Ref. [7]).

Hamiltonian (1) is solved by MC simulations with Arrhenius dynamics, which has been proven efficient in studying relaxation process through spin-flip in spin-crossover materials [19]. A sample of size $L = 100$ is considered with periodic boundary conditions. Let us denote by $P(\{s\},t)$ the probability to find the system in the state $\{s\} = (s_1,\ldots,s_N)$ at time t. This probability evolves in the course of the time following the master equation:

$$\frac{\partial P(\{s\},t)}{\partial t} = -\sum_{j=1}^{N} W_j\left(s_j \to s_j'\right) P(\{s\}_j, s_j, t) + \sum_{j=1}^{N} W_j\left(s_j' \to s_j\right) P\left(\{s\}_j, s_j', t\right) \quad (2)$$

where $\{s\}_j$ denotes the configuration of all spins excepted s_j; $W_j(s_j \to s_j')$, the probability per unit time for transition from the configuration $\{s\}_j$ to $\{s'\}_j$. These transition rates, W, must fulfill the detailed balance condition. In the simulation procedure, one lattice site is randomly chosen. Spin-flip is attempted with the probability:

$$W_j\left(s_j \to s_j'\right) = \frac{1}{3\tau} \exp(-\beta E_j), \quad (3)$$

where $E_j = -Js_j \sum_i s_i - K s_j^2 \sum_i s_i^2 + D s_j^2$ is the change in the system energy associated to the spin-flip move; spins s_i are nearest-neighboring spins of spin s_j and $\beta = \frac{1}{k_B T}$. The frequency $1/\tau$ is defined as follows:

$$\frac{1}{\tau} = \frac{1}{\tau_0} \exp(-\beta E_0^a). \quad (4)$$

The individual spin-flip rate $1/\tau_0$ between the HS and the LS states is fixed here to the value: $2 \times 10^{-3} s^{-1}$. For simplicity, the intermolecular barrier E_0^a is set to zero. The most numerical results presented in the following are obtained by an averaging procedure over 10 to 30 independent runs.

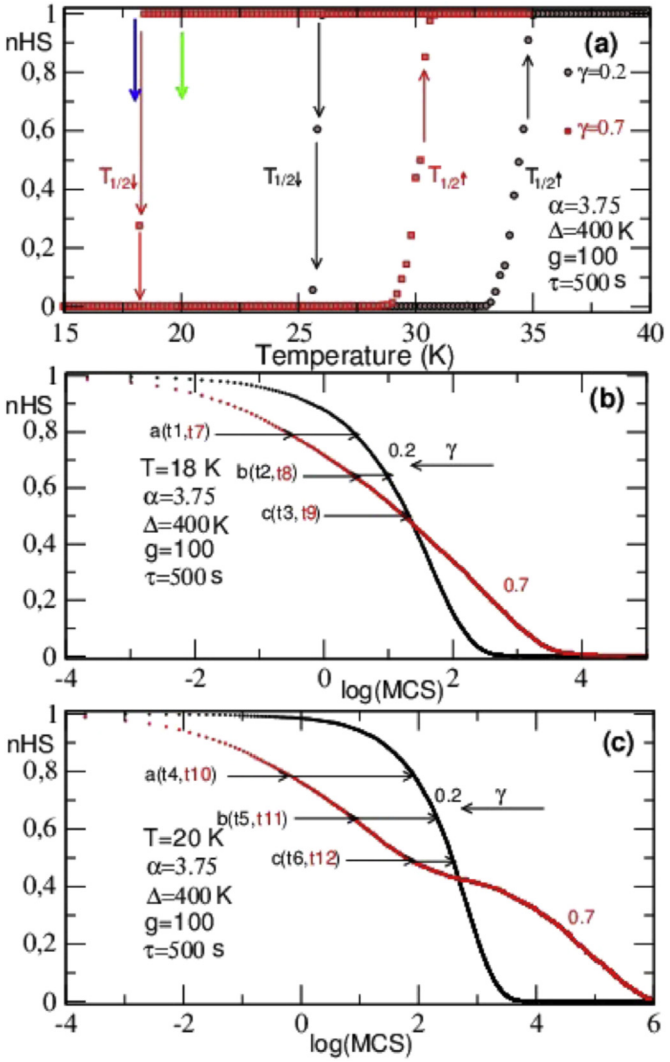

Fig. 1. Thermal hysteresis loops for selected γ values: 0.2 and 0.7 (a). In (b) and (c), sigmoidal isothermal relaxation curves of the system are displayed at low temperatures, $T = 18K$ and $T = 20K$ for the same γ values. Blue and green arrows indicate respectively, the corresponding temperature relaxation in the thermal hysteresis loops (a). For relatively large values of γ, a plateau appears around $n_{HS} = 0.5$ when the temperature T increases as already found in Ref. [21]. Values considered for other parameters are: $\Delta = 400K$; $g = 100$; $\alpha = 3.75$ and $\tau_0 = 500s$. (For interpretation of the references to colour in this figure legend, the reader is referred to the web version of this article.)

3. Results and discussions

3.1. LS units and island statistics during relaxation

Let us first display the isothermal relaxation curves from metastable HS states and hysteresis loops in the vicinity of the thermally-induced first-order phase transition with hysteresis loop of Fig. 1a for various γ values, and analyze some corresponding snapshots in different physical conditions. For increasing values of the magnetic coupling interaction (γ increases), a plateau appears in the relaxation curve (Fig. 1b and c) around $n_{HS} = 0.5$ induced by the temperature as already obtained in Ref. [21] although this plateau is absent in the thermal hysteresis. Moreover when γ increases, the hysteresis loop shifted to low temperatures e.g. for $\gamma = 0.2$; 0.7. The transition temperatures $T_{1/2}$ are in the range of 34.46 and 30.36 K for the upward branch, 25.79 and 18.33K for the downward one, respectively (see Fig. 1a). Fig. 2 displays the case, $\gamma = 0.2$, corresponding to weak magnetic interactions. The figure shows system configurations at different growth times, and temperatures $T = 18K$ and $T = 20K$. Horizontally, snapshots are obtained at the same coverage or concentration θ ($\theta = n_{LS}$) of LS units. Vertically, they correspond to the same simulation temperature T. At $T = 18K$, one gets sparse and very small aggregates with some isolated LS units at time $t_1 = 1.60$ s. When T is raised to $20K$ at the same coverage θ, there are less islands of LS units and very few isolated LS units (subunits in the following) are seen. This means that energetically, growth of subunits in the metastable HS phase are not favoured at high temperature due to thermal excitations. The LS domains growth occurs essentially at edges of LS islands and islands are larger and more compact outer the hysteresis loop (see Fig. 1a). It emerges that thermal fluctuations are playing a major role, acting as the driving force that governs the LS domains growth. At $t_2 = 2.61s$ and $t_5 = 9.82s$, one gets the same previous observations. At $t_3 = 3.75s$, it appears difficult to say that compact islands exist whereas at $t_6 = 13.03s$, coalescence of large compact islands becomes evident. From the snapshots, one fundamentally remark one growth mode. At low temperature, islands are very small and sparse. At high temperature, near the thermal hysteresis loop, one gets large aggregate of LS units which later coalesce. There, the growth essentially occurs at island edges where involved energy barriers are smaller. In Fig. 3, γ is set to 0.7. The two temperatures ($T = 18K$; $20K$) are almost within the hysteresis loop (see Fig. 1a). One sees that the system's

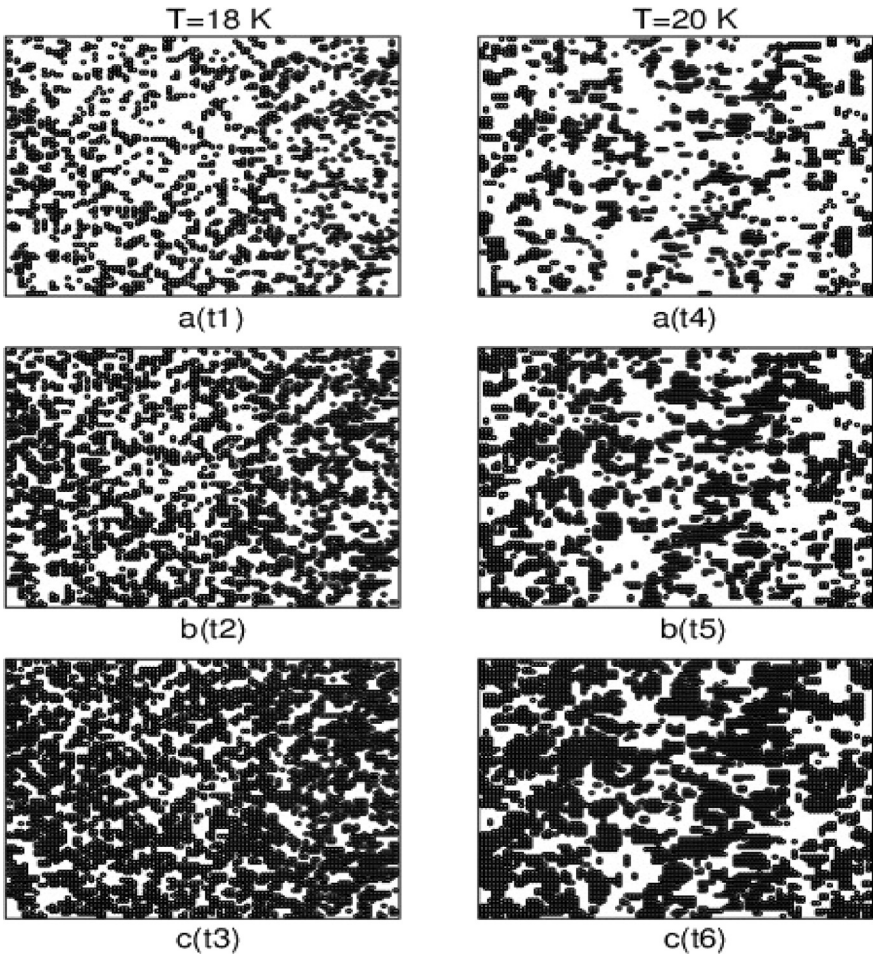

Fig. 2. Snapshots of the system's configurations at two temperatures $T = 18K$ and $T = 20K$ at different growth times $t_1 = 1.60$; $t_2 = 2.61$; $t_3 = 3.75$; $t_4 = 6.50$; $t_5 = 9.82$ and $t_6 = 13.03s$ for $\gamma = 0.2$. Black points represent LS state and white regions are HS phase. Horizontal panels correspond to the same coverage θ ($\theta = n_{LS}$). Vertical panels correspond to the same temperature. At both temperatures, LS nuclei are formed. They grow and coalesce at high coverage. Here growth occurs essentially at LS island edges as in a 2D-nucleation process. In (a), (b) and (c), respectively 20; 35 and 50 percents of the lattice are occupied by LS states. Values considered for other parameters are: $\Delta = 400K$; $g = 100$ and $\alpha = 3.75$.

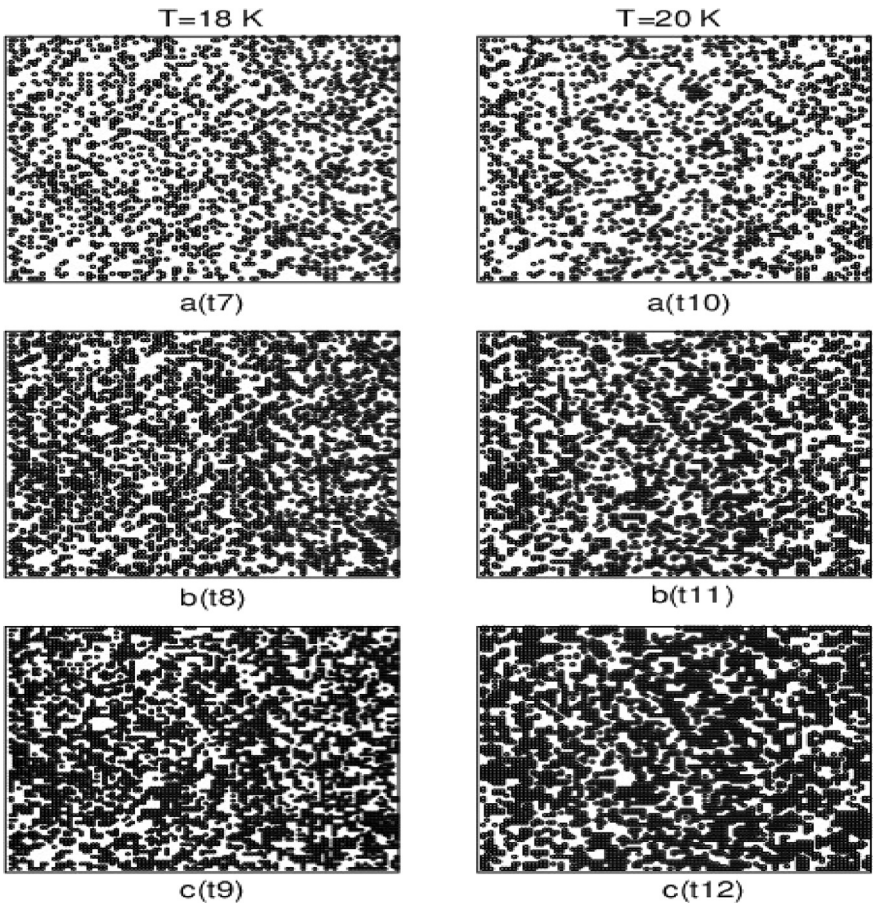

Fig. 3. Snapshots of the system's configurations at two temperatures $T = 18K$ and $T = 20K$ at different growth times $t_7 = 0.57$; $t_8 = 1.56$; $t_9 = 3.45$; $t_{10} = 0.79$; $t_{11} = 2.40$ and $t_{12} = 7.40s$ for $\gamma = 0.7$. Horizontal panels correspond to the same coverage θ. Vertical panels correspond to the same temperature. At both temperatures, LS nuclei are formed. They grow and coalesce at high coverage. Same captions as in Fig. 2. Nucleation of subunits appear everywhere in the system at the early stage of the growth. Islands are very small. Such situation is often observed in continuous crystal growth mode and leads to large fluctuations of the growing crystal surface.

topography is almost the same at the two temperatures where horizontally, panels look similar. One gets sparse and very small aggregates with more isolated LS units. Then, one may conclude that more the magnetic interactions are important (stabilizing the HS state), more we loose the 2*D*-nucleation character of the growth of the LS phase. In other words, an increase of the magnetic interaction at fixed T reduces the 2*D*-nucleation process. Nevertheless, the same phenomenon can be observed probably for weak magnetic interactions (e.g. $\gamma = 0.2$) and within its corresponding thermal hysteresis loop. Then, by rising the temperature T from 25*K* to 26.50*K*, at different relaxation times, the system exhibits also the change in the growth mode of LS domains (see Fig. 4).

Let us now present some statistics of subunits and aggregates at different growth conditions. Fig. 5 quantifies the previous observations on Fig. 2 at LS units coverage $\theta = 0.35$. In fact, for $\gamma = 0.2$, LS subunits density is high at low temperature (panel a). As a consequence, the average LS island size is very small. This clearly shows that the average LS island size appears smaller at $T = 18K$ compared to that at 20*K* as observed in Fig. 2. When T increases, the subunits density decreases and tends to saturate at high temperature. As a result, the LS species have much more time to grow up and to form bigger domains. This is mainly due to the fact that at $T = 20K$, the system is closer to the hysteresis loop (cooling branch) than for $T = 18K$. As found in Fig. 3, the previous observations are valid for $\gamma = 0.7$ as it appears clear from Fig. 5. Numerical results show that the situation is reversed when $\gamma \geq 1.2$. In fact, smaller LS island density is observed at low temperature whereas at high temperature, compact and large aggregates are expected. The value γ' 1.2 appears as a transition point in the behavior of the LS aggregates in the system. One can summarize the different observations as follows. For $\gamma < 1.2$, numerous small and sparse aggregates are formed at low temperature. On the contrary, at high temperature, few aggregates with large size are got. They extend by receiving at their edges new subunits and finally coalesce in the course of the time. A clear investigation of the three panels of Fig. 5 reveals that the LS aggregate density and their average size become almost independent of γ at high temperatures (e.g. $T = 18$; 20; 23*K*). It is instructive to check how the growth proceeds in the course of the time when $\theta\,(= 1-n_{HS})$ increases. This is shown in Figs. 5 and 6. In Fig. 6, for $\gamma = 0.2$, the subunits density increases up to a maximum that depends on the temperature and then decreases exponentially to zero towards the layer completion ($\theta = 1$). The LS aggregates density behaves similarly. A sigmoidal decay of this density is observed after the maximum. Since the subunits coverage is an increasing function of growth time, one can now realize that the sigmoidal decay of the n_{HS} fraction obtained in Refs. [20,21] may be related to the behavior of the LS aggregates density. For $\theta > 0.05$, the behavior of the aggregates density and

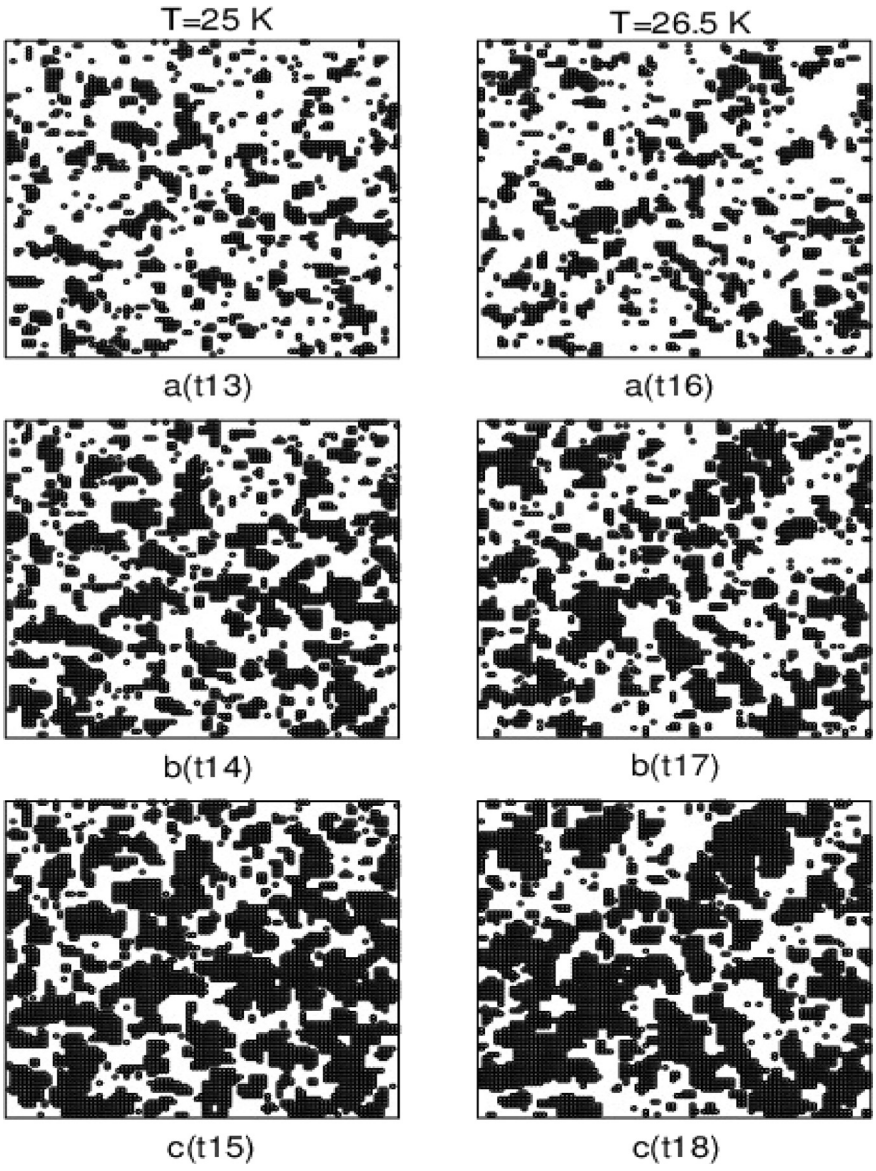

Fig. 4. Snapshots of the system's configurations at two temperatures $T = 25K$ and $T = 26.5K$ at different growth times $t_{13} = 341.00$; $t_{14} = 501.54$; $t_{15} = 649.08$; $t_{16} = 924.82$; $t_{17} = 1411.61$ and $t_{18} = 1867.63s$ for $\gamma = 0.2$. Horizontal panels correspond to the same coverage θ. Vertical panels correspond to the same temperature. At both temperatures, LS nuclei are formed. They grow and coalesce at high coverage. Same captions as in Fig. 2. Nucleation of subunits appear everywhere in the system at the early stage of the growth. Islands are very small. This behavior is similar to what is found in Fig. 3.

average size fundamentally change and depend on T up to a very large coverage. At relatively large coverage, few aggregates with large size exist and a 2D-nucleation takes place. The maxima observed in the density curves are associated to the onset of LS islands coalescence. The corresponding critical coverages are weakly independent on T, but strongly depend on γ (Figs. 6 and 7). In Fig. 7, the system is investigated in the case where magnetic interactions become important with respect to biquadratic (K) "phonons" contribution. In that case, the average size of LS aggregate increases with temperature at relatively large coverage θ. The LS islands density decreases almost exponentially with the coverage, at least up to $\theta = 0.65$ after the maximum (see Fig. 7a; b). One detects a critical coverage θ_c ' 0.45 around which the behavior of the LS aggregates statistically changes.

3.2. The LS aggregate growth modes and phase diagram

Now, let us justify that in some physical conditions, the aggregates grow via 2D-nucleation. The 2D-nucleation mechanism is the layer-by-layer growth mode observed during the multilayer growth of a perfect crystalline surface. It may proceed either by the birth and spread of supercritical nuclei or by the birth and spread of a single aggregate. The latter is commonly referred to as the one-cluster mode [2]. In the layer-by-layer crystal growth, a layer tends to be completed before a new one

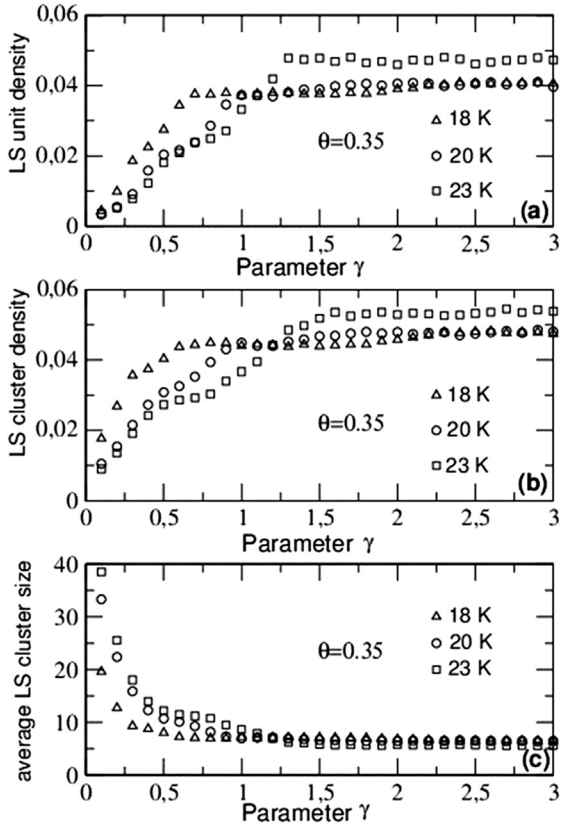

Fig. 5. LS units and islands statistics at coverage $\theta = 0.35$, $T = 18$; 20; 23K as functions of the parameter γ. At low values of γ, few islands with large size exist. Growth proceeds by 2Dnucleation. On the contrary, at large values of γ, numerous LS aggregates with small size exist and a continuous growth mode is suspected. (a): LS units density formation. (b): LS cluster density. In panels (a) and (b) these densities are increasing function of γ (see text). (c): Average LS cluster size as a function of γ at fixed temperature T. Values considered for other parameters are: $\Delta = 400K$; $g = 100$; $\alpha = 3.75$ and $\tau_0 = 500s$ [21].

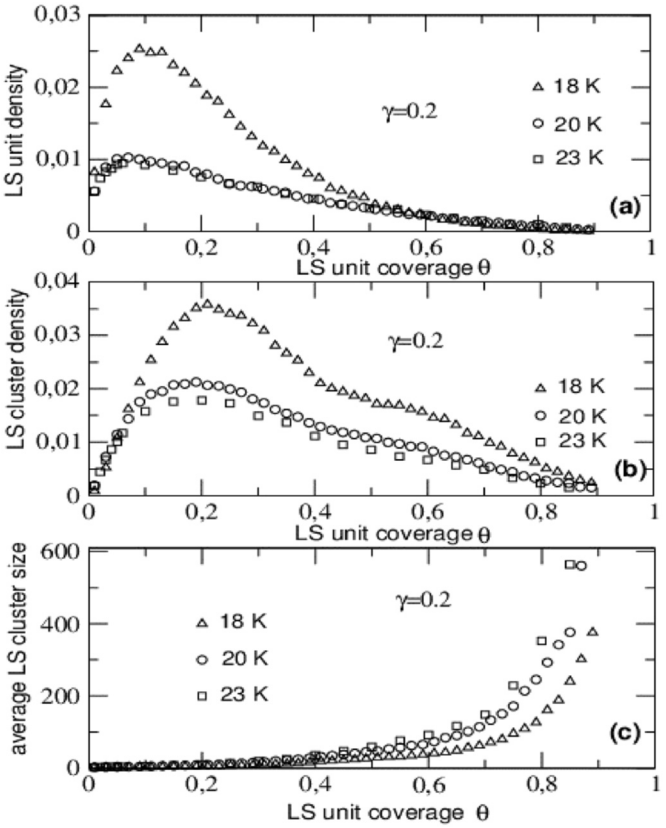

Fig. 6. LS units and islands statistics as function of the coverage θ ($\theta = n_{LS}$) for three temperatures marked on the curves and $\gamma = 0.2$. The LS units density already saturates at $T = 20K$ (panel a). The maximum of the LS island density is associated to the onset of islands coalescence (panel b). At low temperature, islands size are very small at low coverage. The corresponding coverage is almost T-independent but depends on γ (see Fig. 7). Values considered for other parameters are: $\Delta = 400K$; $g = 100$; $\alpha = 3.75$ and $\tau_0 = 500s$ [21].

is started on it. In this regime, when growth occurs from vapor or a supersaturated solution, the growth rate or velocity may be proportional to the nucleation rate: $\exp(-C/\Delta\mu)$ where C is $\Delta\mu$-independent. It may follow the Becker-Doering law: $G = f(\beta, E_s, \Delta\mu)\exp(-\beta E_s^2/3\Delta\mu)$. There, $\Delta\mu$ denotes the change in the chemical potential between the fluid and the crystalline phases, $\beta = \frac{1}{k_B T}$ where T the absolute temperature. E_s is the step energy per unit length which is a decreasing function of temperature and f is the so-called Zeldovich prefactor. $E_s(T)$ may vanish at the roughening temperature T_R of the crystalline surface at equilibrium ($\Delta\mu = 0$). In the present relaxation model of LS islands growth, T is playing as derived from Figs. 2–5, the role of a driving force for the aggregates growth. Let us remind the reader that γ also depends on T and that γT behaves as J/α. By analogy, we calculate an average growth rate or velocity of the LS state defined by the equation: $G \simeq \frac{n_{HS} - \tilde{n}_{HS}}{t_g}$ where n_{HS} is the HS fraction at the initial stage, t_g the relaxation time until $\tilde{n}_{HS} = 0.01$. Below $\tilde{n}_{HS}$, the relaxation becomes extremely slow. Three selected values of α are considered (see Fig. 8) for the computation of G as a function of γ. In all three panels, the growth rate increases, goes through a maximum and then decreases. In the following, we show that the increasing parts of the curves describe a "layer-by-layer"-like mode: birth, extension and coalescence of supercritical LS aggregates. The exponential decreasing part may be related to a "continuous growth" described by the Wilson-Frenkel law (see Ref. [2]). There, nucleation of subunits should occur everywhere in the system as observed for $\gamma = 0.7$ in Fig. 3. This feature, is similar to the early stage of the multilayer growth of a 2D-crystal. Now, let us try to extract a certain island "edge energy" E_s to confirm the 2D-nucleation limited growth character during the increasing part of G. We plot the logarithm of G function at each temperature T as a function of $1/\beta\gamma$ as in Fig. 4 of Ref. [2]. By analogy, γ is playing here the role of $\Delta\mu$. Numerical analysis indicate that the best logarithm function reads: $\ln(G/(1/\beta\gamma))$. This is done in Fig. 9a and yields curves best-fitted to straight lines. The slopes of these lines enable to evaluate E_s^2. For $T = 18$; 20 and 22K, E_s is evaluated as 0.09; 0.10 and 0.11K, respectively. Further investigations of the dynamics are needed to substantiate the true behavior of E_s with T. One is however able now to define some "edge energy" which features the 2D-nucleation growth. Let us remark from Fig. 8 that the maximum growth rate corresponding to the onset of continuous growth mode featured by nucleation of sparse subunits in the system, depends on the temperature and other parameters like α. Indeed, α influences the growth rate and also shifts the onset of continuous growth mode of the LS phase to

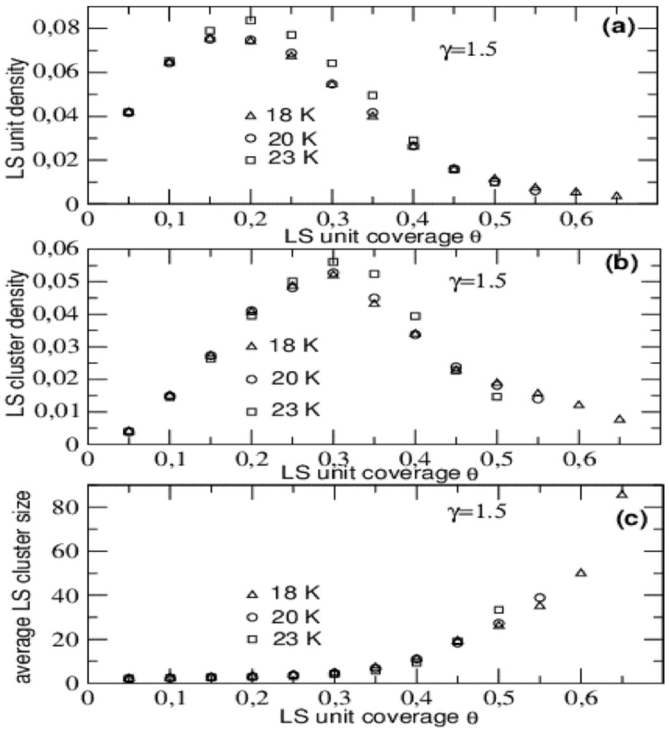

Fig. 7. LS units and islands statistics as function of the coverage θ ($\theta = n_{LS}$) at three different temperatures $T = 18K$ (triangles), $T = 20K$ (circles) and $T = 23K$ (squares) for $\gamma = 1.5$. Up to $\theta = 0.5$, the results look quantitatively and qualitatively almost similar.

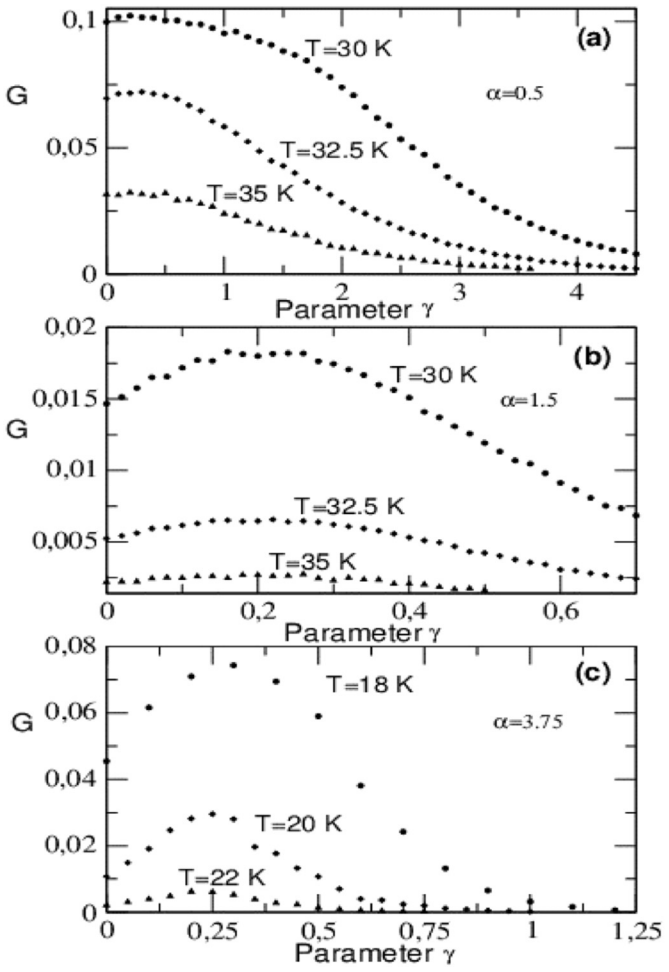

Fig. 8. Average growth velocity of the LS phase as a function of γ for three different values of the parameter α: 0.5 (a); 1.5 (b); 3.75 (c) and different temperatures (see panels). The growth velocity presents a maximum after which it decreases. The value of γ associated with the maximum is a decreasing function of T. In a crude approximation, based on the main exponential factor in the Becker-Doering law (see text), this maximum may be taken as a transition point between the 2D-nucleation growth mechanism and the continuous growth mode of the LS phase inside the SC materials. Values considered for other parameters are: $\Delta = 400K$; $g = 100$ and $\tau_0 = 500s$ [21].

lower values of γ. Using values of γ (denoted γ_c) corresponding to the maximum growth rate, we constructed a schematic growth phase diagram for the LS aggregate during relaxation from the metastable HS phase. This is however a crude approximation that is based on the main exponential factor of G in the Becker-Doering law. The growth phase diagram is done by the transition line drawn in Fig. 9b. Below this line, nucleation and growth occur at few sites and proceed via the 2D-nucleation mode. Above, nucleation of subunits appear everywhere in the system. In crystal growth, such situation may generate a continuous mode with large fluctuations of the growing crystalline surface. Let us remark that this growth phase diagram bears strong resemblance with those found in Ref. [2]. In addition, finite phase diagram temperatures would also confirm their validity in the thermal hysteresis loop.

These studies allow us to substantiate the different LS phase growth mechanisms involved during the relaxation process. Two interacting remarks emerge. The first one is the key role played by the temperature T as a driving force which induced thermal spin-transition. The second one is that of the self-acceleration played by the parameter γ when the magnetic interaction propagates within the system.

4. Conclusion

We investigated by means of MC simulation, the spatio-temporal properties of a cooperative 2D SC and PBAs compounds described by the BEG Hamiltonian during their relaxation from the HS metastable state to the LS state at various temperatures. The nucleation of LS units appeared stochastically in the system. The LS units and islands statistics have been studied for selected values of the model parameters. In some growth conditions of the LS phase, 2D-nucleation mechanism is recovered. Few LS islands are formed, grow and coalesce to cover all the system. We have calculated numerically the edge free energies of these aggregates and realized that they are temperature-dependent. In another region of the model parameters, the growth mechanism appeared different and proceeded via the nucleation of numerous and sparse LS subunits in the early stage of the growth. In crystal multilayer growth, this may later generates mounds and valleys. Using values associated to the maximum growth rate at each temperature, we constructed the growth phase diagram of the system. Other calculations are under way to check whether the subunits and aggregates density and the average aggregate size have some universality behaviors. For extensions in progress: we look

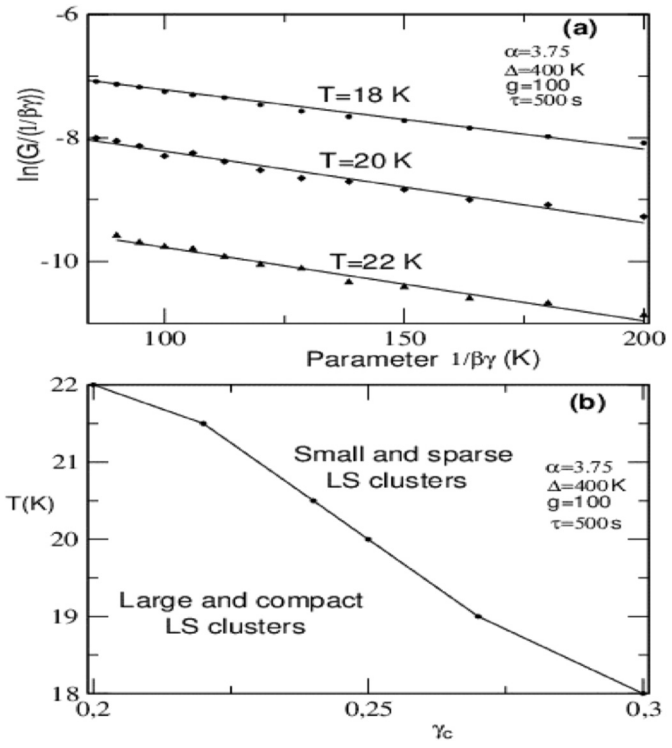

Fig. 9. Panel (a): Plot of $\ln(G/(1/\beta\gamma))$ as a function of $1/\beta\gamma$ at different temperatures as labeled on the curves and $\alpha = 3.75$. The linear character of the curves indicates that the LS domains growth in these regions proceeds via 2*D*-nucleation. Panel (b): schematic growth phase diagram using values of γ associated to maxima of the growth velocity (see Fig. 8c) as transition points between two growth modes. Below the transition line, growth does proceed by 2*D*-nucleation. Above, LS units nucleated everywhere in the system.

forward to study growth mode inside the thermal hysteresis; including long-range interactions to mimic the elastic coupling between the spin states.

References

[1] F.F. Abraham, in: Homogeneous Nucleation Theory, Academic, New-York, 1974.
[2] F. Hontinfinde, M. Touzani, Surf. Sci. 338 (1995) 236.
[3] Y. Ishibashi, Y. Takagi, J. Phys, Soc. Jpn. 31 (1971) 506.
[4] Y.N. Ovchinnikov, I.M. Sigal, Phys. Rev. B 48 (1993) 1085.
[5] P.A. Rikvold, B.M. Gorman, Cond-Mat/9407027 (July 1994).
[6] U.T. Ndongmouo, E. Houngninou, F. Hontinfinde, Surf. Sci. 601 (2007) 672.
[7] T.D. Oke, F. Hontinfinde, K. Boukheddaden, Eur. Phys. J. B 86 (2013) 271 and references therein: K. Boukheddaden, S. Miyashita, and M. Nishino, Phys. Rev. B 75 (2007) 094112.
[8] H. Tokoro, S.-I. Ohkoshi, K. Hashimoto, Appl. Phys. Lett. 82 (2003) 1245.
[9] F. Varret, K. Boukheddaden, C. Chong, A. Goujon, B. Gillon, J. Jeftic, A. Hausser, Eur. Phys. Lett. 77 (2007) 30007.
[10] Y. Ogawa, T. Ishikawa, S. Koshihara, K. Boukheddaden, F. Varret, Phys. Rev. B 66 (2002) 073104.
[11] A. Hausser, Coord. Chem. Rev. 111 (1991) 275.
[12] C. Mottet, R. Ferrando, F. Hontinfinde, A.C. Levi, Surf. Sci. 417 (1998) 220.
[13] J.A. Stroscio, D.T. Pierce, Phys. Rev. B 49 (1994) 8522.
[14] Y.W. Mo, J. Kleiner, M.B. Webb, M. Lagally, Phys. Rev. Lett. 66 (1991) 1998.
[15] S. Jain, Monte Carlo Simulations of Disordered Systems, World scientific Publishing Co. Pte. Ltd, 1992.
[16] K. Binder, D.W. Heermann, Monte Carlo Simulation in Statistical Physics, fifth ed., Springer-Verlag Berlin Heidelberg, 2010. DOI:10.1007/978-3-642-03163-2.
[17] J.A. Venables, G.D. Spiller, M. Hanbuecken, Rep. Prog. Phys. 47 (1984) 399.
[18] P. Jensen, H. Larralde, A. Pimpinelli, Phys. Rev. B 55 (1997) 2556.
[19] K. Boukheddaden, I. Shteto, B. Hôo, F. Varret, Phys. Rev. B 62 (2000) 14796. K. Boukheddaden, ibid. 62 (2000) 14806 and references therein.
[20] M. Nishino, K. Boukheddaden, S. Miyashita, F. Varret, Phys. Rev. B 68 (2003) 224402 and references therein.
[21] T.D. Oke, F. Hontinfinde, K. Boukheddaden, J. Appl. Phys. A (2015), http://dx.doi.org/10.1007/s00339-015-9189-x.